The Tandem Repeat Domain in the *Listeria monocytogenes* ActA Protein Controls the Rate of Actin-based Motility, the Percentage of Moving Bacteria, and the Localization of Vasodilator-stimulated Phosphoprotein and Profilin

Gregory A. Smith,* Julie A. Theriot,‡ and Daniel A. Portnoy*

*Department of Microbiology, University of Pennsylvania, School of Medicine, Philadelphia, Pennsylvania 19104-4318; and ‡Whitehead Institute, Cambridge, Massachusetts 02142

Abstract. The ActA protein is responsible for the actin-based movement of *Listeria monocytogenes* in the cytosol of eukaryotic cells. Analysis of mutants in which we varied the number of proline-rich repeats (PRR; consensus sequence DFPPPPTDEEL) revealed a linear relationship between the number of PRRs and the rate of movement, with each repeat contributing ~2–3 μm/min. Mutants lacking all functional PRRs (generated by deletion or point mutation) moved at rates 30% of wild-type. Indirect immunofluorescence indicated that the PRRs were directly responsible for binding of vasodilator-stimulated phosphoprotein (VASP) and for the localization of profilin at the bacterial surface. The long repeats, which are interdigitated between the PRRs, increased the frequency with which actin-based motility occurred by a mechanism independent of the PRRs, VASP, and profilin. Lastly, a mutant which expressed low levels of ActA exhibited a phenotype indicative of a threshold; there was a very low percentage of moving bacteria, but when movement did occur, it was at wild-type rates. These results indicate that the ActA protein directs at least three separable events: (*1*) initiation of actin polymerization that is independent of the repeat region; (*2*) initiation of movement dependent on the long repeats and the amount of ActA; and (*3*) movement rate dependent on the PRRs.

Listeria monocytogenes is a Gram-positive facultative intracellular bacterial pathogen that grows in the cytosol of eukaryotic cells (12, 47). During intracellular growth, *L. monocytogenes* moves in the host cytosol and spreads cell to cell by a mechanism dependent upon the polymerization of host actin (8, 24, 36, 45, 47). When first exposed to the cytosolic environment of the host, *L. monocytogenes* becomes coated uniformly in a network of actin filaments and actin-binding proteins referred to as an actin "cloud" (47). The cloud rearranges into an asymmetric structure, or actin "tail," at the onset of bacterial actin-based movement (36, 45, 47). The force for movement is presumably provided by actin polymerization at the interface of the actin tail and the surface of the bacterium (36, 45). The actin tail does not move with the bacterium but is fixed in the cytosol and depolymerizes at a constant rate. Thus, the length of the actin tail is proportional to the rate at which the bacterium is moving (45).

Address all correspondence to Dr. Daniel A. Portnoy, Department of Microbiology, University of Pennsylvania, School of Medicine, Abramson Center, Rm 804, 34th Street and Civic Center Blvd., Philadelphia, PA 19104-4318. Tel.: (215) 898-8913. Fax: (215) 573-9068. E-mail: portnoy@pobox.upenn.edu

L. monocytogenes has been measured moving at speeds up to 87.6 μm/min in the J774 mouse macrophage-like cell line and 24 μm/min in the PtK2 potoroo kidney epithelial cell line (8, 45). Moving bacteria often interact with the host plasma membrane, forming stable filopod-like projections with a single bacterium at the filopod tip (24, 47). Mutants unable to induce actin polymerization do not induce filopod formation, are incapable of cell-to-cell spread, and are avirulent (3, 9, 17).

Unraveling the mechanisms that control actin polymerization in living cells is complicated by the large array of actin-binding proteins and the involvement of membranes in both the regulation and induction of actin polymerization (30, 54). *L. monocytogenes* provides a simplified model for the study of actin polymerization, as actin-based motility can be reconstituted in cell-free extracts (46). In addition, *L. monocytogenes* provides a genetic model in which a single surface-exposed protein, ActA, is sufficient to induce both actin polymerization and actin-based motility (19, 38).

ActA is a 639–amino acid transmembrane protein with no overall identity to other known proteins. However, ActA contains two interdigitated sets of repeats (see Fig. 1 *a*) (9, 17). The smaller repeats are 11 amino acids in length

and consist of three or four consecutive prolines surrounded by four acidic amino acids. Each "proline-rich repeat" is separated from its neighbor by one of three sequences collectively called the "long repeats." The first two long repeats are 24 amino acids in length and are 92–100% identical depending upon the isolate of *L. monocytogenes* (Smith, G.A., and D.A. Portnoy, unpublished observations). The third long repeat is composed of 33 amino acids that share no sequence identity with the first two long repeats. However, all three long repeats are predicted to have similar hydrophilic and secondary structure profiles (Smith, G.A., and D.A. Portnoy, unpublished observations).

The number of functions the ActA protein performs to generate bacterial motility is unknown. In the simplest scenario, ActA may provide free barbed ends of filamentous actin (either by a filament trapping, uncapping, severing, or "de-novo" nucleation event) and the reaction conditions of the host cell may spontaneously polymerize actin into filaments and propel the bacteria through the cytoplasm (23). However, the isolation of a *L. monocytogenes* mutant that polymerizes actin but fails to move suggests that the induction of actin-based motility may be more complex (20). Mutational analysis of ActA has been performed in bacterial-free plasmid-based mammalian cell transfection systems (11, 28). By this approach, an NH_2-terminal region of ActA separable from the repeats was implicated in initiating actin polymerization, while the region of ActA including the repeats enhanced the amount of actin polymerized (29). While such models allow for easy manipulation of the *actA* gene, they are limited in that they only reproduce the process of actin polymerization and are not functional for the study of actin-based motility. More recently, mutated ActA isoforms have been expressed in *L. monocytogenes* from a multicopy plasmid (21). These studies have corroborated the findings of the transfection experiments and went on to show that removal of the entire repeat region of ActA results in a slower rate of bacterial actin-based motility. Taken together, these studies indicate that the generation of bacterial actin-based motility by the ActA protein is accomplished by multiple functions.

Two cytosolic host eukaryotic proteins have been implicated to play a direct role in the actin-based motility of *L. monocytogenes.* The first identified, profilin, is a poly-L-proline and monomeric actin binding protein (42, 44). The second, vasodilator-stimulated phosphoprotein (VASP),[1] is a profilin binding protein (13, 34). Both proteins have been demonstrated to localize at the bacterial/actin–tail interface of moving *L. monocytogenes*, the site where actin polymerization is known to occur (5, 46). Additionally, VASP has been shown to directly bind the ActA protein (5). The binding sites responsible for this interaction are not known on either protein; however, large deletions within ActA that span both NH_2-terminal and COOH-terminal of the repeat motifs fail to bind VASP (29). The functional significance of this interaction and the effects of these deletions on association with profilin are unknown.

In this study, ActA function has been evaluated using strains of *L. monocytogenes* expressing a series of sequential deletions and mutations within the ActA repeat motifs. The results demonstrate a quantitative role for the proline-rich repeats in the localization of VASP and profilin at the bacteria/tail interface and the rate of actin-based motility. In addition, the long repeats, in a mechanism that is independent of VASP/profilin binding, enhance the transformation of actin polymerization into a force-generating mechanism capable of propelling *L. monocytogenes* through the cytosol in a directional manner.

Materials and Methods

Bacterial Strains and Culture Conditions

Two wild-type isolates of *L. monocytogenes* were used in this study. 10403S, used in the majority of these experiments, expresses very limited amounts of ActA while in bacterial growth media and has an LD_{50} value in BALB/c mice of $\sim 2 \times 10^4$ (32). The hyper-hemolytic isolate, SLCC-5764, expresses constitutively high levels of ActA and was used for all studies involving *Xenopus laevis* cytoplasmic extracts. All in-frame deletions in the chromosomal *actA* gene were introduced into 10403S, as described below. A subset of these deletions were introduced into SLCC-5764 for examination in cell-free extracts.

All strains were grown in brain/heart infusion broth (BHI; Difco Laboratories Inc., Detroit, MI), and maintained on BHI agar. Stock cultures were stored at −80°C in 50% (vol/vol) glycerol/BHI broth.

Construction of L. monocytogenes Mutant Strains

All *actA* in-frame deletion constructs were first subcloned into *Escherichia coli* DH5α (Bethesda Research Laboratories Life Technologies, Inc., Gaithersburg, MD) on the shuttle plasmid pKSV7 (39). Maintenance of pKSV7 in *E. coli* was achieved with 50 μg of ampicillin/ml of growth media. In *L. monocytogenes*, 10 μg of chloramphenicol/ml of growth media was used to maintain pKSV7. The Δ*actA1* allele was generated by amplifying the 10403S chromosomal *actA* gene by PCR. Primers used were 5′GGAATTCATTACTGCCAATTGCATTA3′, which is derived from bases 43–61 (relative to the *actA* open reading frame), and 5′GGTCTAGATCAAGCACATACCTAG3′, which is derived from sequence downstream of the *actA* open reading frame. The product was ligated into pKSV7 using EcoRI- and XbaI-generated DNA ends, resulting in pDP2117. Plasmid pDP2117 was digested with SacI, which had two recognition sequences endogenous to the *actA* sequence. (The two SacI restriction sites were identical counterparts within each long repeat encoding sequence.) The digested plasmid was self-ligated, resulting in pDP2118. Transformation of 10403S with pDP2118 was performed by electroporation as previously described, and allelic exchange was used to replace the chromosomal wild-type *actA* allele with the plasmid borne Δ*actA1* allele as previously described (4), resulting in strain DP-L2157.

All other in-frame deletions were generated using the technique of splicing by overlap extension (SOEing) PCR (16). Briefly, for each deletion a pair of complementary primers were designed containing an equal amount of a sequence identity to sequence both 5′ and 3′ of the region to be deleted. These primers were first used separately in conjunction with an additional primer either 5′ or 3′ of the deletion. The resulting amplified products shared identity at one end, originating from the complementary primers. A secondary amplification was then performed using an equal molar ratio of the two PCR products as template and the same 5′ and 3′ primers. The resulting amplified product possessed the desired deletion and was cloned into pKSV7 for allelic exchange in 10403S. Complementary primers used were as follows: 5′AATGCTTCGGACTTCCCACCGCCTCCAACA3′ and its complement for the generation of Δ*actA2*, 5′AGCTCATTCGAATTTCCACCAATCCCAACA3′ and its complement for the generation of Δ*actA3*, 5′AATGCTTCGGACTTCCCACCAATCCCAACA3′ and its complement for the generation of Δ*actA4*, 5′TACGGATGAAGAGTTAAACGGGAGAGGCGGT3′ and its complement for the generation of Δ*actA5*, and 5′GAGGTAAATGCTTCGAACGGGAGAGGCGGT3′ and its complement for the generation of Δ*actA6*. The upstream primers used in the above SOEing reactions were 5′GGGAATTCTGAAGCTTGGGAAGCAG3′, which is derived from sequence upstream of the *actA* open reading frame, and 5′GGT-

1. *Abbreviations used in this paper*: BHI, brain/heart infusion broth; PtK2, potoroo kidney epitelial cells; SOE, splicing overlap extension; VASP, vasodilator-stimulated phosphoprotein.

CTAGATCAAGCACATACCTAG3′, which is derived from sequence downstream of the *actA* open reading frame. 10403S chromosomal DNA was used as template for all initial reactions, with the exception of those used in the construction of Δ*actA3*, which used DP-L2157 chromosomal DNA. All final SOEing amplified products were ligated into pKSV7 using EcoRI- and XbaI-generated DNA ends resulting in pDP2237 (Δ*actA2*), pDP2291 (Δ*actA3*), pDP2292 (Δ*actA4*), pDP2321 (Δ*actA5*), and pDP2322 (Δ*actA6*). All plasmids were independently transformed into 10403S and allelic exchange was performed resulting in strains DP-L2270 (Δ*actA2*), DP-L2300 (Δ*actA3*), DP-L2301 (Δ*actA4*), DP-L2373 (Δ*actA5*), and DP-L2374 (Δ*actA6*). Additionally, SLCC-5764 was transformed with pDP2321 and pDP2322, and allelic exchange resulted in strains DP-L2742 and DP-L2823, respectively.

The Δ*actA3-K*, Δ*actA3-G*, and Δ*actA3-GG* alleles were also generated using the SOEing PCR method. In each case, a pair of complementary primers were designed with identity to a sequence encoding a proline-rich repeat but with point mutations resulting in the desired amino acid substitutions. Thus, for the generation of Δ*actA3-G*, 5′GTAAATGCTTCGGACTTCGGGGGAGGAGGTACGGATGAAGAGTTAAGA3′ and its complement were used. For the generation of Δ*actA3-K*, 5′CCCGCCACCACCTACGAAAAAGAAGTTAAGACTTGCTTTGCCA3′ and its complement were used. For the generation of Δ*actA3-GG*, 5′CCGAGCTCATTCGAATTTGGCGGCGGCGGAACAGAAGAAGAGTTGAAC3′ and its complement were used. The 5′ primer used in these reactions was 5′GGAAGCTTGTGGATGCTTCTGAAAGTGAC3′, which is derived from bases 544–564 (relative to the *actA* open reading frame). The 3′ primer used in these reactions was 5′GGGTCGACTTACGCATTTCTTGAGTGTTTTC3′, which is derived from bases 1301–1320 (relative to the *actA* open reading frame). DP-L2300 chromosomal DNA was used as the primary template for the construction of Δ*actA3-G* and Δ*actA3-K* alleles, and DP-L2656 (see below) chromosome was used for the generation of Δ*actA3-GG*. The final products were ligated into pKSV7 using HindIII- and SalI-generated DNA ends resulting in pDP2641, pDP2642, and pDP2963, respectively. Each plasmid was independently transformed into 10403S and allelic exchange was performed resulting in strains DP-L2656 (Δ*actA3-G*), DP-L2657 (Δ*actA3-K*), and DP-L2990 (Δ*actA3-GG*). All engineered deletions and mutations were confirmed by sequencing.

Tissue Culture and Immunofluorescence Microscopy

Four cell lines were used in this study. The J774 mouse macrophage-like cell line was used for metabolic labeling of ActA during intracellular infection (see below). The phagocytic properties of this cell line allowed for maximal infection, which was beneficial for these experiments. J774 cells were grown and maintained as previously described (32). Potoroo kidney epithelial (PtK2) cells were used for video microscopy, and Hela cells were used for immunofluorescence microscopy. Both cell lines have flat cell morphologies, which are beneficial in these applications. Additionally, antiprofilin and anti-VASP antisera were human specific, necessitating the use of the Hela cells. PtK2 and Hela cells were grown and maintained as previously described (45, 46). L2 cells were used in plaque assays and were grown and maintained as previously described (41).

Double immunofluorescence of profilin and filamentous actin was as previously described (46). Affinity-purified rabbit anti–human profilin antiserum was a gift of Dr. Pascal Goldschmidt-Clermont (10). Double immunofluorescence of VASP and filamentous actin was performed by the same methods, but with the following exceptions: Primary antibody was affinity purified rabbit anti-VASP antisera made against the synthetic peptide CEAFVQELRKRGSP (derived from the COOH-terminal protein sequence of the human VASP protein), and was kindly provided by Dr. Tim Mitchison (University of California, San Francisco, CA) and Dr. Matt Welch (University of California, San Francisco). Lissamine rhodamine-conjugated donkey anti–rabbit immunoglobulin was used as secondary antibody (Jackson ImmunoResearch Labs, Inc., West Grove, PA), in conjunction with fluorescein-phalloidin (Molecular Probes, Eugene, OR) to visualize filamentous actin. Coverslips were mounted in Vectashield (Vector Laboratories Inc., Burlingame, CA).

Metabolic Labeling of ActA during Infection and SDS-PAGE

Labeling of ActA during intracellular infection was derived from the method of Headley and Payne (14), and was essentially as previously described (3). Briefly, J774 cells were infected with 10^7 bacteria grown overnight in BHI at 30°C. This resulted in a multiplicity of infection of two bacteria per J774 cell. The cells were washed with PBS and given fresh culture media (DME + 7.5% fetal bovine serum) lacking methionine 30 min after infection. 1 h after infection, 50 μg gentamicin/ml culture media was added, and 30 μg anisomycin plus 225 μg cycloheximide/ml culture media were added at 3.25 h after infection. Labeling of ActA with 450 μCi [^{35}S]methionine (Trans^{35}S-label; ICN Biomedicals, Inc., Costa Mesa, CA)/ml culture media was begun at 3.5 h after infection and continued for 1 h, at which time cells were lysed in 2× final sample buffer (2% SDS, 0.06 M Tris, pH 6.8, 10% glycerol, 0.05% bromophenol blue) and boiled for 5 min. Approximately one-third of each sample was subjected to SDS-PAGE (8% acrylamide) and the resulting gel was processed for fluorography (EN^{3}HANCE; DuPont New England Nuclear, Wilmington, DE).

Video Microscopy and Image Analysis

All video recordings were performed on an inverted microscope (Diaphot 300; Nikon Inc., Melville, NY) equipped with phase-contrast and epifluorescence optics. Infected cells on 25-mm-round glass coverslips were maintained at 37°C using an aluminum chamber connected to a circulating water bath. Images were acquired using a camera (Newvicon; Hamamatsu Corp., Bridgewater, NJ) and image processing software (Metamorph; Universal Imaging Corporation, West Chester, PA). Images were stored on optical disc (Panasonic, Secaucus, NJ). For movement rate measurements, time-lapse sequences were recorded by capturing one video frame every 10 s. Bacterial speed was determined by averaging the distance moved every 10 s over a 1-min interval. Movement frequency was determined by counting the total numbers of moving and stationary bacteria in infected cells during a 3-min time window. Between 10 and 20 host cells were counted for each bacterial strain; standard deviations represent cell-to-cell variation.

Plaquing and Virulence Assays

Infection and plaque formation in a confluent monolayer of L2 cells was as previously described (41). Briefly, L2 cells were infected with 6×10^6 bacteria in six-well tissue culture trays (Costar Corp., Cambridge, MA). Infected cells were incubated for 1 h and then washed with PBS. The infected cells were then immediately overlaid with 3 ml DME containing 5% fetal bovine serum, 0.7% agarose, and 10 μg gentamicin/ml overlay. Cells were incubated for another 3–4 d and then stained with neutral red to visualize viable cells. The diameters of individual plaques were measured as previously described (37). The LD_{50} for BALB/c mice injected intravenously was performed as previously described (32).

Extract Preparation and Detection of Bacterial Motility

Cytostatic factor-arrested (meiotic) cytoplasmic extracts of *X. laevis* eggs were prepared as previously described (46). Bacterial strains were grown overnight at 37°C in BHI, rinsed and resuspended in *Xenopus* extract buffer (25), and incubated with cytoplasmic extract on ice for 1 h before examination on the microscope.

Results

Generation of L. monocytogenes actA In-Frame Deletion Mutants

A series of in-frame deletions were designed to examine the function of the repeat motifs of the ActA protein. Our goal was to remove specific regions of ActA without affecting the overall structure and folding of the protein. Because tandem proline residues have been postulated to form flexible helical structures that may act as spacers between distinct domains of a protein (52), the deletions were designed to maintain the context of the proline-rich repeats within the flanking sequences of the protein. All deletions were introduced into the chromosomal *actA* gene of *L. monocytogenes* by allelic exchange to assure the correct expression and regulation of the *actA* constructs (Fig. 1 *b*).

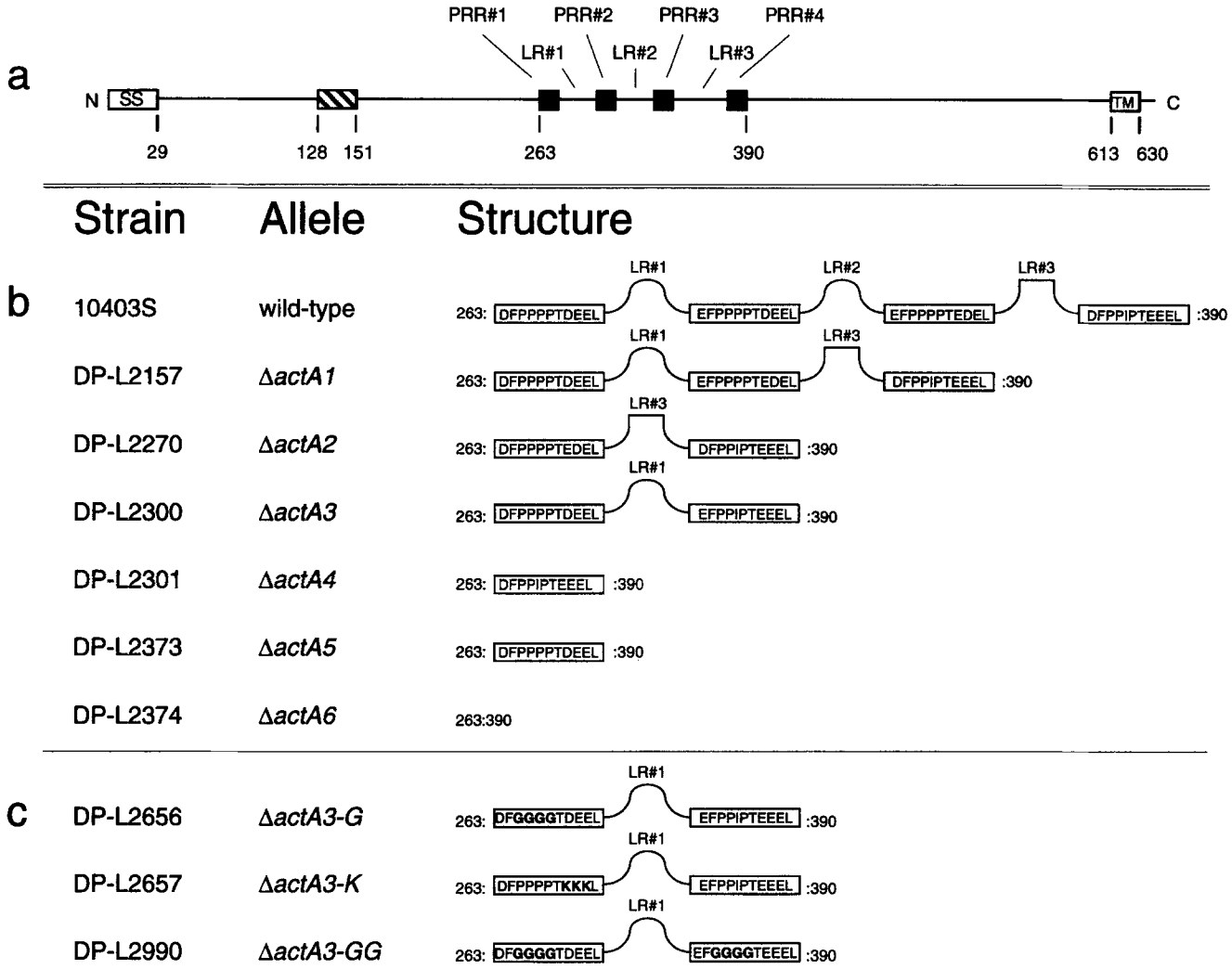

Figure 1. Schematic representation of chromosomal *actA* gene products. (*a*) Entire ActA protein. (*b*) Wild-type and in-frame deletion isoforms. (*c*) Mutated isoforms derived from the Δ*actA3* allele. Only the region of the proteins from amino acids 263–390 are shown in *b* and *c*. *SS*, signal sequence; *TM*, transmembrane domain; *stipled box*, region required for actin polymerization (29); *PRR*, proline-rich repeat (shown as sequences in rectangles in *b* and *c*); *LR#1*, first long repeat; *LR#2*, second long repeat; *LR#3*, third long repeat (which lacks sequence similarity to LR#1 and LR#2, but is referred to as a "long repeat" because of similarities to LR#1 and LR#2 in hydrophilicity, surface probability, and juxtaposition relative to the proline-rich repeats). Amino acid changes resulting from directed mutation within the proline-rich repeats are emphasized in bold. Long repeats are not shown to scale in *b* and *c*.

The resulting strains invaded and grew in J774 cells normally (data not shown) and expressed the mutant forms of the ActA protein in the host cytoplasm at levels equivalent to wild type when assayed by [^{35}S]methionine incorporation (Fig. 2 *A*). Each of the major protein bands labeled in Fig. 2 *A* were further confirmed to be ActA with ActA specific antiserum (data not shown). Migration of ActA in SDS-PAGE is anomalous for two reasons. First, the wild-type ActA protein resolves into three distinct protein bands, which we have previously demonstrated to be a result of protein phosphorylation (3). The Δ*actA1* protein migrates as two bands, while the Δ*actA2* protein migrates as one. These observations are consistent with residues in the first two long repeats being specific sites for phosphorylation. (The Δ*actA3* protein runs as two closely migrating bands that are not resolved in Fig. 2; data not shown.) The role of this phosphorylation will be the subject of a separate report. Second, the mature wild-type ActA protein is predicted to encode a 67-kD protein yet migrates in SDS-PAGE with an apparent molecular mass of 97 kD (bottom band). This is probably at least partially accounted for by the high content of proline in ActA (35). Each truncated ActA isoform migrates proportionately less aberrantly than wild-type ActA protein approximately relative to percent proline content.

The Repeat Motifs Enhance Actin-based Motility

Unlike strains of *L. monocytogenes* lacking all ActA function (3, 9, 17), all the strains presented in this study were found to induce the polymerization of host actin at the bacterial surface in the form of actin clouds and actin tails. PtK2 cells were infected with each strain for 4 h and examined by video microscopy. Approximately 80% of wild-

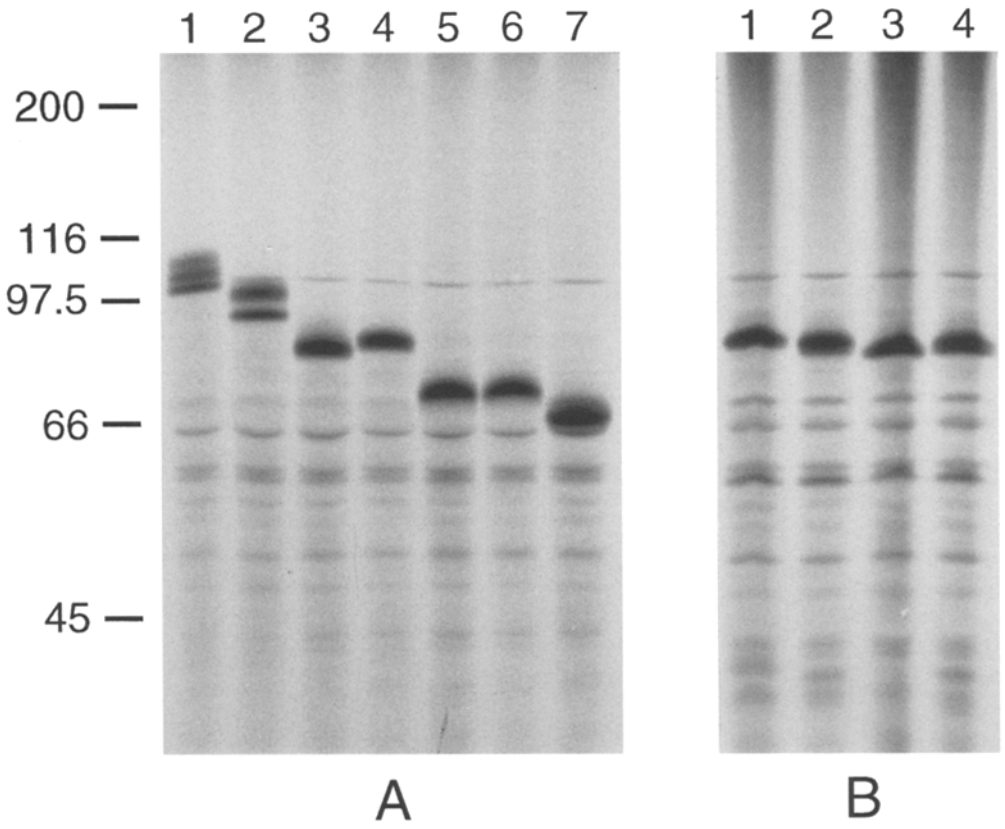

Figure 2. Expression of ActA during intracellular infection. Proteins were labeled with [^{35}S]methionine during infection of J774 cells, harvested, and run through 8% SDS-PAGE, followed by fluorography. (*A*) Wild-type and in-frame deletion isoforms. Lane *1*, wild type; lane *2*, Δ*actA1*; lane *3*, Δ*actA2*; lane *4*, Δ*actA3*; lane *5*, Δ*actA4*; lane *6*, Δ*actA5*; lane *7*, Δ*actA6*. (*B*) Isoforms expressed from the Δ*actA3* strain and strains with the derivative alleles. Lane *1*, Δ*actA3*; lane *2*, Δ*actA3-K*; lane *3*, Δ*actA3-G*; lane *4*, Δ*actA3-GG*. Numbers at left represent molecular weight markers in kD.

type *L. monocytogenes* were moving in any given 3-min interval, consistent with previous observations (45). The Δ*actA1*–Δ*actA3* strains moved at frequencies similar to wild type. In contrast, strains having only one proline-rich repeat (Δ*actA4* and Δ*actA5*) or lacking the entire repeat region (Δ*actA6*) moved much less frequently than wild type (Fig. 3 *a*). Lack of actin-based motility was not due to a lack of actin polymerization, as the majority of Δ*actA4*–Δ*actA6* bacteria were associated with "actin caps" when examined as fixed samples. The actin caps were asymmetrically located at one bacterial pole, yet unlike actin tails they did not appear to extend from the bacterial surface (Figs. 4 *G* and 5 *D*).

Bacteria in the process of actin-based motility were also measured for rate of movement. Of the subset of bacteria that were moving, the wild-type strain moved at an average speed of 14.2 μm/min and a top speed of 30 μm/min, which is in agreement with rates previously reported in PtK2 cells (45). Strikingly, the strain lacking the entire repeat region of ActA (Δ*actA6*), moved at rates approximately threefold slower than wild type. The remaining deletion strains (Δ*actA1*–Δ*actA5*), all harboring deletions smaller than Δ*actA6*, moved at rates intermediate between wild type and the Δ*actA6* strain. Taken together, the strains showed a trend in which movement rates were inversely proportional to the size of the deletion in each *actA* allele (Fig. 3 *b*). A strain expressing an isoform of ActA derived from Δ*actA5* in which the single proline-rich repeat was disrupted by the insertion of six additional prolines also moved at rates nearly identical to Δ*actA6* (data not shown).

The Repeat Motifs Mediate Association with VASP and Profilin

The VASP protein binds directly to ActA, and association of VASP with *L. monocytogenes* is dependent upon a region of ActA that includes the repeat motifs (5, 29). We examined VASP association with the deletion strains by indirect immunofluorescence after infection of Hela cells. Wild-type bacteria were associated with an asymmetric distribution of VASP as previously described (Fig. 4) (5). The deletion strains associated with amounts of VASP correlating to the size of the chromosomal *actA* deletion. The presence of the first or third long repeat did not appear to affect VASP association, as the Δ*actA2* and Δ*actA3* strains were similar or identical to each other. VASP association was detectable with bacteria expressing only one proline-rich repeat (Δ*actA4* and Δ*actA5*) but was not detectable in the strain lacking the entire repeat region (Δ*actA6*). In general, association of VASP with motile bacteria appeared to be greatest at the bacterial pole adjacent to the actin tail and decreased along the sides of each bacterium until undetectable at the opposing pole. This asymmetric gradient of VASP was evidenced by the lack of VASP detection along the sides of bacteria harboring the larger in-frame deletions, with the Δ*actA4* and Δ*actA5* strains binding only a punctate patch of VASP at one pole.

VASP also binds directly to profilin (34), which in turn was reported to be required for *L. monocytogenes* actin-based motility (46). We therefore examined association of profilin with the deletion strains by indirect immunofluorescence. As previously described, profilin associates with

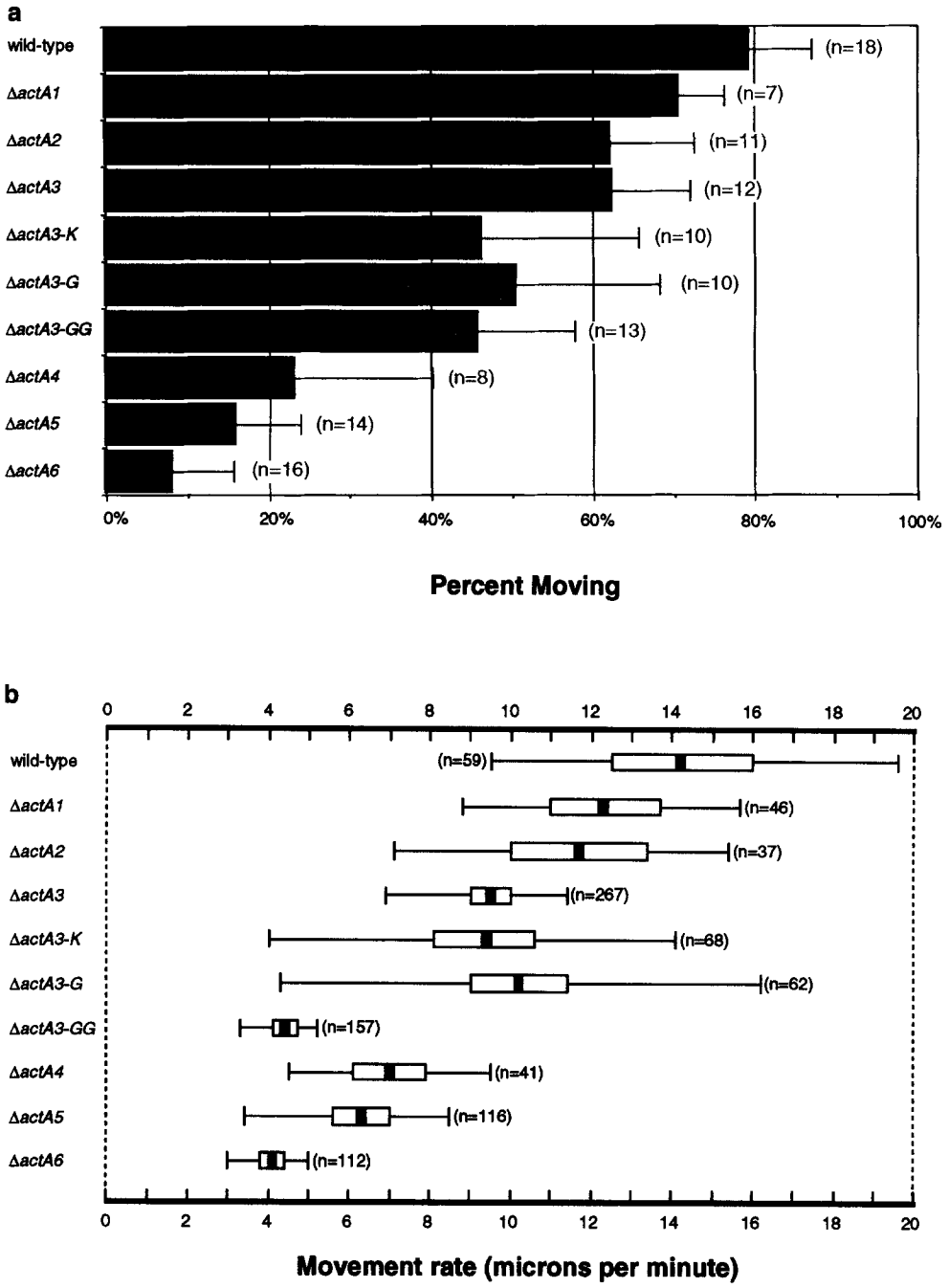

Figure 3. Frequency and rates of *L. monocytogenes* motility during PtK2 intracellular infection. (*a*) Bar graph illustrating percent of *L. monocytogenes* moving 4 h after infection. Error bars represent standard deviations between infected cells, with *n* values equal to the number of cells counted. Between 30 and 100 bacteria were examined per infected PtK2 cell. (*b*) "Box and Whiskers" plot of *L. monocytogenes* movement rates. Black rectangles are the means, white rectangles are 95% certainty limits for the means, and the whiskers are the intraquartile ranges (from the 25th to the 75th percentile). *n* values equal number of bacteria measured. All of the mutant rates passed a normality test.

the wild-type *L. monocytogenes* in an asymmetric distribution (46). Profilin association with the deletion strains was similar to VASP association in three ways. First, the localization of profilin with bacteria correlated to the size of the *actA* deletion in each strain. However, colocalization of profilin was limited to the smallest three in-frame deletions (Δ*actA1*–Δ*actA3*). Profilin association was not detected with strains having only one proline-rich repeat (Δ*actA4* and Δ*actA5*) or lacking the entire repeat region (Δ*actA6*) (Fig. 5 and data not shown). Second, the Δ*actA2* and Δ*actA3* strains appeared to associate with profilin equally, indicating the first and third long repeats were interchangeable in this regard (data not shown). Third, profilin associated with bacteria in an asymmetric gradient similar to VASP. With wild-type bacteria, profilin was observed all around the bacteria except at the pole opposite the actin tail. This was clearly observed in dividing bacteria, in which this pole was at the septum (Fig. 5 *A*). In the Δ*actA2* and Δ*actA3* strains, profilin localization was limited to a punctate spot at the bacterial pole associated with the actin tail.

Mutagenesis of the Proline-rich Repeats

As previously stated, the repeat region of ActA is composed of an interdigitated series of repeats: the four proline-rich repeats and the three long repeats. To determine which repeats were responsible for VASP and profilin association as well as enhanced actin-based motility, we altered the proline-rich repeats of the chromosomal Δ*actA3*

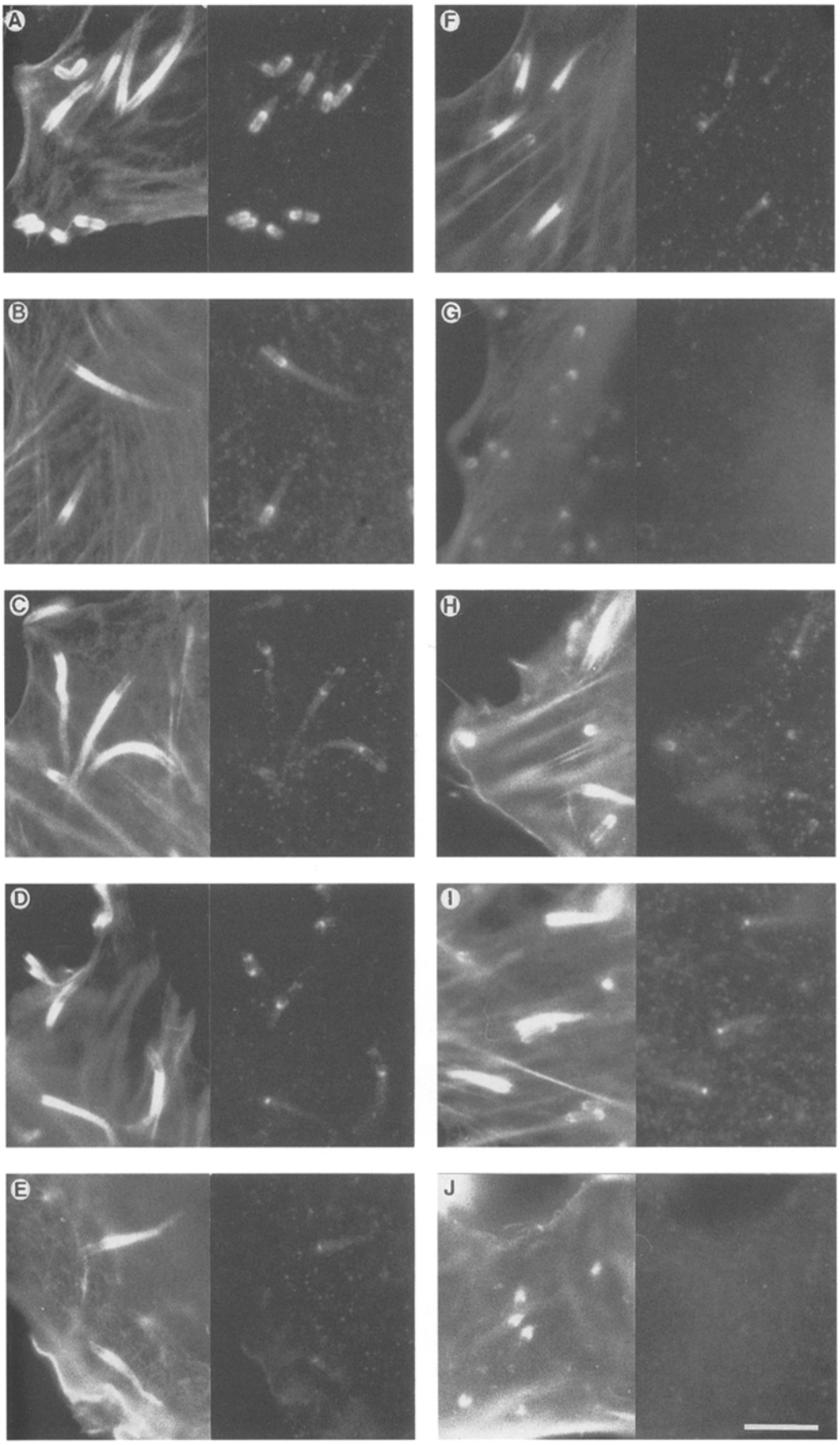

Figure 4. Immunolocalization of VASP with *L. monocytogenes* in Hela cells. F-actin (*left*) and VASP detection (*right*) were of the same field for each sample. VASP was visualized with affinity purified anti-VASP antiserum specific to a peptide derived from the human VASP sequence. F-actin was visualized with phalloidin.

(*A*) 10403S (wild type); (*B*) DP-L2157 (Δ*actA1*); (*C*) DP-L2270 (Δ*actA2*); (*D*) DP-L2300 (Δ*actA3*); (*E*) DP-L2301 (Δ*actA4*); (*F*) DP-L2373 (Δ*actA5*); (*G*) DP-L2374 (Δ*actA6*); (*H*) DP-L2656 (Δ*actA3-G*); (*I*) DP-L2657 (Δ*actA3-K*); (*J*) DP-L2990 (Δ*actA3-GG*). Bar, 5 μm.

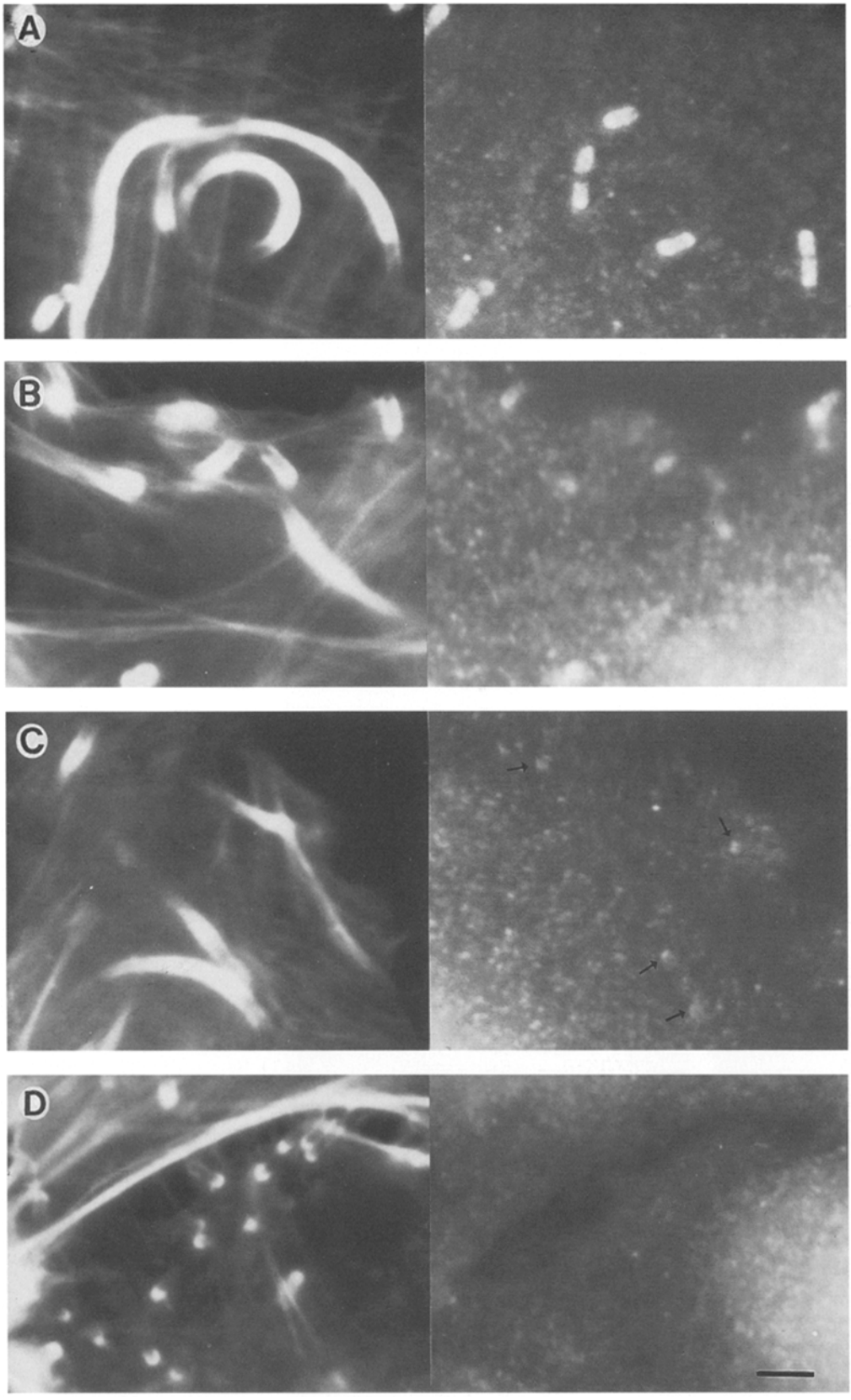

Figure 5. Immunolocalization of profilin with *L. monocytogenes* in Hela cells. F-actin (*left*) and profilin (*right*) detection were of the same field for each sample. Profilin was visualized with affinity purified anti-human profilin. F-actin was visualized with phalloidin. (*A*) 10403S (wild type); (*B*) DP-L2157 (Δ*actA1*); (*C*) DP-L2300 (Δ*actA3*); (*D*) DP-L2374 (Δ*actA6*). *Arrows*, dim profilin patches associated with DP-L2300 (Δ*actA3*). Bar, 3 μm.

allele by site-specific mutagenesis. We examined the contribution of the proline-rich repeats in the context of the Δ*actA3* allele more closely for two reasons. First, Δ*actA3* only possesses two proline-rich repeats, thus minimizing the amount of targeted mutagenesis required to address their function. Second, defects in percent moving were only noted in strains expressing isoforms of ActA with less than two proline-rich repeats (Fig. 3 *a*). We first generated

two strains expressing alleles of Δ*actA3* with mutations in the first proline-rich repeat alone: Δ*actA3-G* and Δ*actA3-K* (Fig. 1 *c*). In the Δ*actA3-G* allele, the four adjacent prolines of the first repeat were replaced with four glycines, while the Δ*actA3-K* allele had three adjacent acidic residues (DEE) replaced with three lysines. These mutant isoforms of ActA were stable and expressed normally during infection of J774 cells (Fig. 2 *B*). Both mutant strains were found to move at frequencies and rates equivalent to the Δ*actA3* parent (Fig. 3, *a* and *b*), and appeared associated with an amount of VASP equal to or greater than the Δ*actA4* and Δ*actA5* strains (Fig. 4). The role of the proline-rich repeats was further addressed by generating a derivative of the Δ*actA3-G* allele in which both proline-rich repeats possessed the substitution of four glycines for the four prolines (Fig. 1 *c*). Like the Δ*actA6* strain, the Δ*actA3-GG* strain did not associate with VASP (Fig. 4). Furthermore, the Δ*actA3-GG* strain had the surprising mixed phenotype of moving at rates equivalent to the Δ*actA6* strain, but at frequencies approaching the wild-type and Δ*actA1*–Δ*actA3* strains (Fig. 3, *a* and *b*).

Virulence of the Mutant Strains

The virulence of each mutant strain was determined by mouse LD_{50} and plaque formation in confluent monolayers of L2 cells (Table I). Increases in LD_{50} were only observed with strains lacking all three long repeats (Δ*actA4*–Δ*actA6*). The LD_{50} was not notably affected by mutations within the proline-rich repeats (Δ*actA3-K*, Δ*actA3-G*, and Δ*actA3-GG*); however, in the absence of all three long repeats, the presence of one proline-rich repeat was beneficial (compare Δ*actA6* with Δ*actA4* and Δ*actA5*). In the plaque formation assay, decreases in plaque size were noted with strains lacking either all three long repeats or having less than two proline-rich repeats (Fig. 6). Thus, the plaque formation assay was more sensitive to losses in proline-rich repeats than was the LD_{50} assay. This was most apparent with the Δ*actA3-GG* strain, which was indistinguishable from wild type by LD_{50} assay, but similar to the Δ*actA5* strain by plaque formation assay.

Bacterial Motility in Cell-free Extracts

The role of profilin in the actin-based motility of *L. monocytogenes* has been directly addressed in cell-free cytoplasmic extracts derived from *X. laevis* oocytes (23, 46). Because the 10403S isolate of *L. monocytogenes* expresses the ActA protein only during the course of intracellular infection and not in extracts, we introduced two of the deletion alleles, Δ*actA5* and Δ*actA6*, into the chromosome of a hyper-hemolytic strain (SLCC-5764) that expresses ActA constitutively. As with the PtK2 infections, only motile bacteria were measured to compute average movement rates. Similar to what was observed in PtK2 cells, bacteria expressing the Δ*actA5* and Δ*actA6* alleles moved at slower rates than the wild-type strain. However, the Δ*actA5* and Δ*actA6* strains did not move at rates significantly different from each other (Table II).

Properties of a Mutant with Decreased Expression Of Wild-Type ActA

We have previously described a mutant of *L. monocytogenes* harboring a transposon insertion in the promoter region of the *prfA* gene (strain DP-L973) (41). This strain expresses decreased levels of the PrfA-regulated gene products, including ActA (Smith, G.A., and D.A. Portnoy, unpublished observations). Video microscopy of PtK2 cells infected with this strain revealed that, similar to the strain harboring the Δ*actA6* allele, only 10.2% (SD = .048, n = 16) of the bacteria were moving. In contrast to the in-frame deletion strains, decreased expression of ActA did not result in slower movement rates for those bacteria undergoing actin-based motility, as the subset of bacteria that were motile moved at an average speed of 13.63 μm/min (SD = 6.68, n = 25), similar to the wild-type strain.

Discussion

The *L. monocytogenes* ActA protein is necessary and sufficient to produce actin-based motility when present in an asymmetric distribution around a bacterial surface (3, 9, 17, 19, 38). While the mechanism by which ActA functions

Table I. LD_{50} of L. monocytogenes Strains with Summary of Mutant Phenotypes

Strain	*actA* allele	Percent moving*	Average rate of movement*	VASP‡	Profilin‡	Plaque size	Mouse LD_{50}
			μm/min				
10403S	Wild type	79%	14.2	++++	++++	100%	$\sim 2 \times 10^4$
DP-L2157	Δ*actA1*	71%	12.3	+++	++	97%	$< 1 \times 10^5$
DP-L2270	Δ*actA2*	62%	11.7	++	+	97%	$< 1 \times 10^5$
DP-L2300	Δ*actA3*	62%	9.5	++	+	101%	$< 1 \times 10^5$
DP-L2301	Δ*actA4*	23%	7.0	+	−	70%	$\sim 1 \times 10^5$
DP-L2373	Δ*actA5*	16%	6.2	+	−	76%	$\sim 1 \times 10^5$
DP-L2374	Δ*actA6*	8%	4.1	−*	−	61%	$\sim 8 \times 10^5$
DP-L2656	Δ*actA3-G*	51%	10.3	+/++	ND	89%	$< 1 \times 10^5$
DP-L2657	Δ*actA3-K*	46%	9.4	+/++	ND	92%	$< 1 \times 10^5$
DP-L2990	Δ*actA3-GG*	46%	4.4	−*	ND	77%	$< 1 \times 10^5$
DP-L973	Wild type Decreased Expression	10%	13.5	ND	ND	ND	ND

*In PtK2 cells (see Fig. 3 for details)
‡VASP and profilin associations with bacteria are approximations based on immunofluorescence images and are not true quantitation.

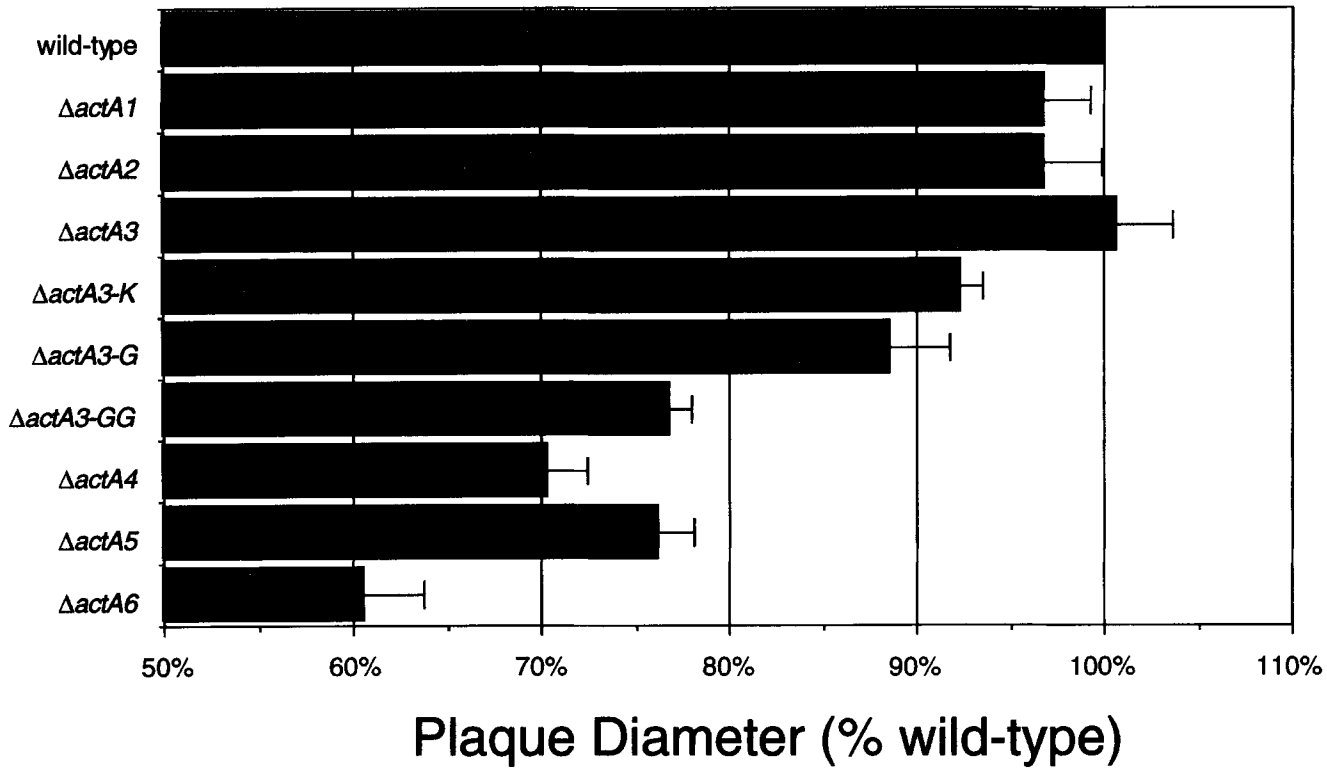

Figure 6. Ability of *L. monocytogenes* to form plaques in monolayers of L2 cells. Bar graph represents plaque size formed by each strain relative to wild type. For each strain, the results of at least three separate experiments were averaged. In each experiment, 10–20 individual plaques were measured per strain and averaged. Error bars represent standard deviations.

is largely unknown, large deletions in the *actA* gene have been used to map regions of the ActA protein responsible for initiating and enhancing actin polymerization and motility (21, 29). In this study, we have performed a detailed examination of the ActA repeat motifs. From this molecular analysis, we provide evidence of at least three functional domains involved in the generation of actin-based motility. These domains are responsible for: (*a*) initiation of actin accumulation, (*b*) harnessing actin polymerization into a motile force, and (*c*) accelerating actin filament elongation and bacterial motility rate.

The Proline-rich Repeats: Acceleration of Actin Filament Elongation and Bacterial Motility

Several observations indicate that the proline-rich repeats mediate the association of VASP with bacteria: (*1*) VASP binds ActA directly, and this interaction is dependent upon the central region of the ActA protein that includes the repeat motifs (5, 29). (*2*) There was a correlation between the number of proline-rich repeats in the expressed ActA isoform and the amount of VASP association to the bacterial strain. (*3*) The long repeats were not required for VASP association as the Δ*actA4* and Δ*actA5* strains, which only have one proline-rich repeat each and no long repeats, colocalized with VASP. (*4*) One long repeat, in the absence of any intact proline-rich repeats (Δ*actA3-GG*), failed to recruit VASP to the bacterial surface. From these observations, we conclude that the ActA proline-rich repeats are the direct binding site for VASP and that the proline residues are an essential constituent of the motif.

Table II. Movement Rates in Cell-free X. Laevis Extracts

Strain	*actA* allele	Average rate of movement*
		μm/min
SLCC-5764	Wild type	4.32 ± 1.14 (n = 27)
DP-L2742	Δ*actA5*	2.89 ± 1.10 (n = 20)
DP-L2823	Δ*actA6*	2.97 ± 0.76 (n = 34)

*In PtK2 cells. Error is standard deviation, with n equal to number of individual bacteria measured.

Similar to VASP binding to ActA, the rate of bacterial motility roughly correlated with the number of intact proline-rich repeats, with each repeat adding ~2–3 μm/min to the basal rate of motility (Table I). Deletion of the entire repeat region (Δ*actA6*) resulted in the slowest movement rates, which were ~30% that of wild type in PtK2 cells. Strikingly similar rates were observed when the two proline-rich repeats of the Δ*actA3* allele were both mutated by changing all proline residues to glycines (Δ*actA3-GG*) and when the single proline-rich repeat of the Δ*actA5* allele was disrupted by the insertion of six additional prolines (data not shown). There was not a perfect correlation between movement rate and number of proline-rich repeats, as the Δ*actA2* strain moved at rates significantly faster than Δ*actA3*, even though both strains had two proline-rich repeats. In addition, the Δ*actA3-K* and Δ*actA3-G* strains moved at rates comparable to Δ*actA3* even though one proline-rich repeat had been mutated. These inconsistencies suggest that the position of the proline-rich repeats

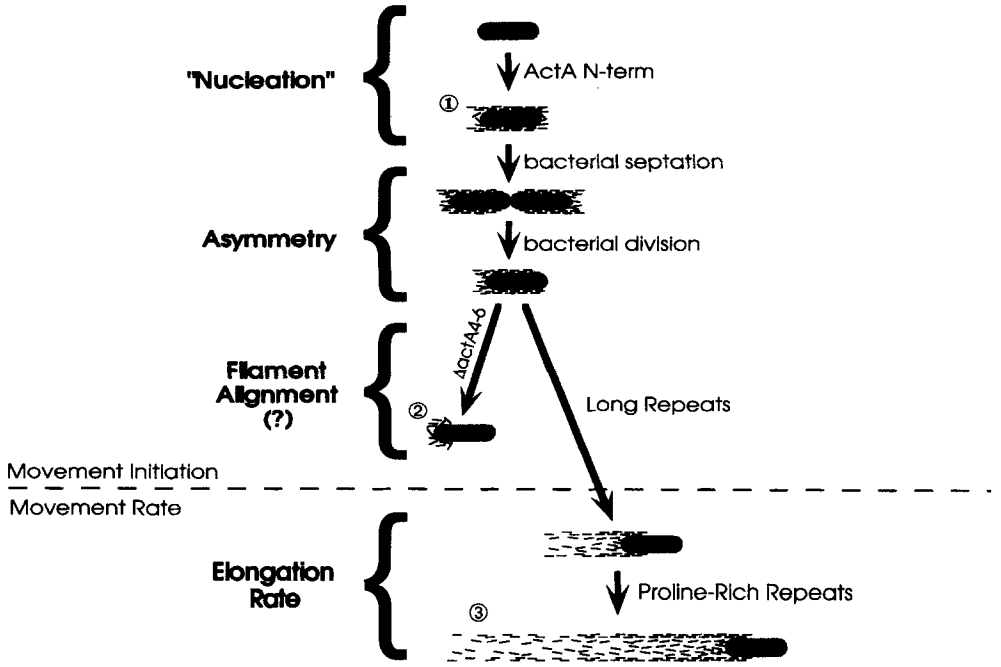

Figure 7. Schematic representation of four independent steps responsible for the generation of bacterial motility. For clarity, steps are shown acting sequentially. Three bacterially associated actin structures are also depicted: circle *1*, actin cloud; circle *2*, actin cap; and circle *3*, actin tail.

relative to the long repeats and the remainder of the ActA protein affect their function.

The mechanism by which the ActA proline-rich repeats accelerate actin-based motility is not clear. ActA does not appear to interact directly with actin (17), implying that the effect of the proline-rich repeats upon actin polymerization is indirect. VASP is likely to be involved in mediating the functions of the proline-rich repeats, as VASP binding to ActA was dependent upon the proline-rich repeats, and the number of proline-rich repeats present in each ActA isoform dictated the amount of VASP associated with bacteria as well as bacterial movement rate. A second host protein implicated in this mechanism is profilin. Profilin has been previously demonstrated to localize to the bacteria and actin tail interface, but this association does not appear to be due to a direct interaction with ActA (46). Similar to VASP, we also observed host profilin to associate with bacteria in a manner that appeared to be dependent upon the number of proline-rich repeats present in the expressed ActA isoform of each strain. This may not be surprising as profilin is a ligand for VASP, and thus VASP may act to tether profilin and ActA together in a protein complex (34).

The contribution of profilin to the actin-based motility of *L. monocytogenes* is a controversial issue. Two reports have directly addressed the role of profilin in the actin-based motility of *L. monocytogenes* by depleting profilin from extracts of *X. laevis* oocytes, which serve as a cell-free model of *L. monocytogenes* actin-based motility (23, 46). In the first report, the depletion of profilin resulted in complete inhibition of bacterial motility, although the bacteria still induced actin polymerization in formations notably similar to the actin cap structures reported here (46). However, the second report found profilin depleted extracts could support movement rates 75–100% that of mock-depleted controls (23). Comparison of these results is complicated by differences in the bacterial strains and extracts used in the two studies. The first report examined the motility of a natural isolate of *L. monocytogenes* in extracts derived from meiotically arrested eggs (46). The second report used a strain of *L. monocytogenes* engineered to express high levels of the ActA protein from a multicopy plasmid and used extracts from activated (interphase) eggs (23). Thus, different factors may have been limiting in the two studies. The Δ*actA6* strain, which fails to associate with VASP and profilin, may provide further insight into these contrasting results. In cell-free extracts, the Δ*actA6* strain moved at rates ~70% that of wild type. However, in PtK2 cells the Δ*actA6* was much more defective, moving at rates ~30% that of wild type with the majority of bacteria associated with actin caps and not moving (Table I). Thus, host factors essential for motility may have been limiting in PtK2 cells but not in our cell-free extracts. Differences in the concentrations of factors such as actin, profilin, and thymosin-β4 are known to exist between different cell types and may account for the differences noted above (22, 26, 27). Differences in host factor concentrations are also very likely responsible for the faster movement rates of the 10403S wild-type strain in J774 cells (87.6 μm/min) compared to that in PtK2 cells (24 μm/min) (8, 45). Similar to different cell types, the motility of *L. monocytogenes* in different batches of cell-free extracts can also vary by at least twofold (23). Because of these batch-to-batch variations and differences in experimental procedure, more direct comparisons will be necessary to accurately address the role of profilin in the cell-free extract system.

This study supports a model in which profilin functions to enhance the actin-based motility of *L. monocytogenes* (44). Profilin likely functions in this regard by increasing the rate of actin elongation at filament barbed ends (27, 33). This is supported by the colocalization of filament barbed ends and profilin at the bacterial/actin-tail interface (46, 49, 50), where profilin may deliver monomeric actin to the

filament barbed ends (27, 33). The barbed ends of the filaments are adjacent to the bacterial pole (49, 50), and thus increased rates of filament elongation result in increased rates of bacterial motility (45).

The Long Repeats: Harnessing Actin Polymerization into a Productive Motile Force

As discussed above, the proline-rich repeats accelerated the rate of actin-based motility. However, strains harboring the larger deletion alleles that lacked all three long repeats (*ΔactA4–ΔactA6*) also displayed significant defects in the percent of moving bacteria. Unlike movement rate and association with VASP and profilin, changes in percent moving did not correlate with the number of intact proline-rich repeats. Instead, this defect was indicative of a threshold. Based on the in-frame deletions, the threshold was crossed either when the expressed ActA isoform had fewer than two proline-rich repeats or had no long repeats. The *ΔactA3-GG* strain, which had one long repeat but no intact proline-rich repeats, exhibited a high percentage of motile bacteria, indicating that the long repeats were the primary functional element enhancing the initiation of actin-based motility subsequent to the induction of actin polymerization. Thus, the long repeats and proline-rich repeats have separable functions, which are both dependent on but separate from the inititiation of actin polymerization. However, it should be noted that the percent moving of the *ΔactA3-GG* strain was less than the wild-type strain, suggesting that the proline-rich repeats may also play some role in enhancing the percentage of moving bacteria.

We hypothesize that the long repeats may function as a homophilic multimerization motif. This hypothesis is based on several indications that the initiation of movement, that is the transduction of actin filament polymerization into bacterial locomotion, is a cooperative event. First, the DP-L973 strain reveals that reduced expression of ActA results in a decreased number of bacteria moving, but when movement does occur it is at wild-type rates. This is the converse of the *ΔactA3-GG* phenotype, where bacteria initiate movement at a frequency near wild type, but at rates drastically reduced from wild type. Second, examination of bacteria immediately after infection shows that bacteria do not initiate movement until after an average of three divisions, but once a bacterium begins movement it moves immediately at full speed (Theriot, J.A., unpublished observations). The simplest model that explains these observations is the requirement of an ActA concentration threshold to initiate movement. One common biological mechanism for generating a concentration threshold for activity is the requirement for subunit multimerization, which here appears to be dependent upon the presence of the long repeats.

While we favor a multimerization model for ActA, this does not explain the mechanism by which the long repeats enhance the initiation of actin-based motility. Work by Zhukarev et al. using fluorescence polarization has demonstrated that the actin filaments present in actin clouds and actin tails are highly ordered in parallel arrays. Actin filament alignment has been postulated to be an essential step in the initiation of actin-based motility, as a mutant of *L. monocytogenes* found associated with actin clouds consisting of unaligned actin filaments does not move (53). By fluorescence polarization, the *ΔactA6* strain polymerized actin filaments with approximately threefold less ordered alignment than wild type (Zhukarev, V., F. Ashton, J.M. Sanger, G.A. Smith, H. Shuman, and J.W. Sanger, unpublished results). We are currently examining whether this defect more precisely correlates with the percent moving defect and the absence of the long repeats. It is provocative to speculate that ActA in a multimerized complex may induce actin organization in parallel arrays, facilitating the initiation of movement.

The Repeat Motifs Are Dispensable for Initiation of Actin Polymerization and Bacterial Actin-based Motility

The region of ActA required to initiate actin polymerization was previously localized to the NH_2 terminus of the protein, distinct from the ActA repeat motifs (21, 29). Consistent with this, all of the ActA isoforms presented in this study initiated host actin polymerization, including the isoform encoded by the *ΔactA6* allele that lacked all the repeat motifs.

While the repeat motifs enhanced actin-based motility, they were not absolutely required for motility. This appears to be in contrast to an earlier study in which microinjected peptide derived from the ActA proline-rich repeat sequence completely inhibited *L. monocytogenes* actin-based motility (40). Based on our data, it is not immediately clear how competitive inhibition of the ActA proline-rich repeats stops motility altogether. The microinjected peptide was noted to produce drastic global effects upon the host cell which may have nonspecifically inhibited motility; alternatively, the peptide may have the interesting property of a dominant negative effect upon a host cell ligand essential for motility.

ActA as a Virulence Factor

ActA contributes to the virulence of *L. monocytogenes* by providing a mechanism by which bacteria can spread cell to cell without encountering the host humoral immune response (31, 48). This strategy is not unique to *L. monocytogenes*, as two unrelated bacterial pathogens, Shigella and *Rickettsia*, as well as a viral pathogen, Vaccinia, all move through the eukaryotic cytosol by apparently similar mechanisms (2, 7, 15, 43). However, only in *L. monocytogenes* and *Shigella* have the proteins directly mediating these processes been identified (6). The *Shigella* protein, IcsA, has no sequence similarity to the ActA protein.

The underlying mechanism by which ActA functions is to induce the polymerization of host actin. Similar to the outgrowth of pseudopodiae and lamellipodiae from eukaryotic cells, actin polymerization itself appears to provide the force necessary to generate bacterial motility (45). In the absence of the ActA repeats, actin polymerization is required and sufficient to direct bacterial actin-based motility and cell-to-cell spread in an L2 plaque formation assay, albeit at reduced efficiency. In the mouse model, a strain of *L. monocytogenes* lacking all ActA function has an LD_{50} of 2×10^7, indicating the virulence is reduced approximately 1,000-fold (3). In contrast, the virulence of the *ΔactA6* strain was 80-fold less than wild type. Thus, the

ability of ActA to promote the virulence of *L. monocytogenes* in the mouse was dramatically enhanced by the repeat motifs. Both the proline-rich repeats (compare the LD_{50} values of Δ*actA5* and Δ*actA6*) and the long repeats (compare the LD_{50} values of the Δ*actA3-GG* and Δ*actA6*) contributed to the enhanced virulence (Table I).

A Step-by-Step Model for the Induction of Actin-based Motility by the ActA Protein

The results of this and other studies indicate that there are at least four separate steps mediating ActA-directed actin-based motility (Fig. 7). The first step is the initiation of actin filament accumulation around the bacteria, which is directed by a domain in ActA NH_2-terminal of the repeats (21, 29). The mechanism by which the ActA protein accomplishes this is unknown but may be either due to a filament trapping, uncapping, filament severing, filament capture, or "de-novo" nucleation event (23). Second, an asymmetry in ActA function relative to the bacterium must be established. The ActA protein has been reported to be present on the bacterial surface in an asymmetric distribution (18), and we have previously demonstrated that the activity of ActA at only one pole of a bacterium is a prerequisite for directional motility (38). The mechanism of asymmetric localization of ActA on *L. monocytogenes* is currently unknown but may be established by cell wall dynamics during bacterial growth and division, as noted in other Gram-positive bacteria (38, 51). Third, the polymerization of actin at one pole of the bacterium must be harnessed as a motile force. The long repeats enhance this process by an unknown mechanism that may involve actin filament alignment and the multimerization of the ActA protein. Fourth, movement rate is enhanced by optimizing the rate of actin polymerization. This is mediated by the proline-rich repeats that bind VASP, which in turn concentrates profilin, and presumably actin, at the site of elongation. The synergism of these functions results in bacteria with enhanced abilities to move by actin-based motility, spread cell to cell in a monolayer of L2 cells (and thus form a larger plaque), and kill a mammalian host.

We thank Rarita Roy for assistance with measurement of movement rates, Matt Welch, Tim Mitchison, and Pascal Goldschmidt-Clermont for providing antibodies, and Sally Zigmond, Phil Youngman, Vivianne Nachmias, David Boettiger, Martin Pring, Annemarie Weber, Mitch Sanders, and David Fung for stimulating discussions during the course of the work.

This work was supported by National Institutes of Health grants AI-26919 (D.A. Portnoy) and AI-36929 (J.A. Theriot), and the W.M. Keck Foundation (J.A. Theriot).

Received for publication 22 July 1996 and in revised form 22 August 1996.

References

1. Aullo, P., M. Giry, S. Olsnes, M.R. Popoff, C. Kocks, and P. Boquet. 1993. A chimeric toxin to study the role of the 21 kDa GTP binding protein rho in the control of actin microfilament assembly. *EMBO (Eur. Mol. Biol. Organ.) J.* 12:921–931.
2. Bernardini, M.L., J. Mounier, H. d'Hauteville, M. Coquis-Rondon, and P.J. Sansonetti. 1989. Identification of *icsA*, a plasmid locus of *Shigella flexneri* that governs bacterial intra- and intercellular spread through interaction with F-actin. *Proc. Natl. Acad. Sci. USA.* 86:3867–3871.
3. Brundage, R.A., G.A. Smith, A. Camilli, J.A. Theriot, and D.A. Portnoy. 1993. Expression and phosphorylation of the *Listeria monocytogenes* ActA protein in mammalian cells. *Proc. Natl. Acad. Sci. USA.* 90:11890–11894.
4. Camilli, A., L.G. Tilney, and D.A. Portnoy. 1993. Dual roles of *plcA* in *Listeria monocytogenes* pathogenesis. *Mol. Microbiol.* 8:143–157.
5. Chakraborty, T., F. Ebel, E. Domann, K. Niebuhr, B. Gerstel, S. Pistor, C.J. Temm-Grove, B.M. Jockusch, M. Reinhard, U. Walter, and J. Wehland. 1995. A focal adhesion factor directly linking intracellularly motile *Listeria monocytogenes* and *Listeria ivanovii* to the actin-based cytoskeleton of mammalian cells. *EMBO (Eur. Mol. Biol. Organ.) J.* 14:1314–1321.
6. Cossart, P. 1995. Actin-based bacterial motility. *Curr. Opin. Cell. Biol.* 7: 94–101.
7. Cudmore, S., P. Cossart, G. Griffiths, and M. Way. 1995. Actin-based motility of vaccinia virus. *Nature (Lond.).* 378:636–638.
8. Dabiri, G.A., J.M. Sanger, D.A. Portnoy, and F.S. Southwick. 1990. *Listeria monocytogenes* moves rapidly through the host-cell cytoplasm by inducing directional actin assembly. *Proc. Natl. Acad. Sci. USA.* 87:6068–6072.
9. Domann, E., J. Wehland, M. Rohde, S. Pistor, M. Hartl, W. Goebel, M. Leimeister-Wächter, M. Wuenscher, and T. Chakraborty. 1992. A novel bacterial virulence gene in *Listeria monocytogenes* required for host cell microfilament interaction with homology to the proline-rich region of vinculin. *EMBO (Eur. Mol. Biol. Organ.) J.* 11:1981–1990.
10. Finkel, T., J.A. Theriot, K.R. Dise, G.F. Tomadelli, and P.J. Goldschmidt-Clermont. 1994. Dynamic actin structures stabilized by profilin. *Proc. Natl. Acad. Sci. USA.* 91:1510–1514.
11. Friederich, E., E. Gouin, R. Hellio, C. Kocks, P. Cossart, and D. Louvard. 1995. Targeting of *Listeria monocytogenes* ActA protein to the plasma membrane as a tool to dissect both actin-based cell morphogenesis and ActA function. *EMBO (Eur. Mol. Biol. Organ.) J.* 14:2731–2744.
12. Gaillard, J.L., P. Berche, J. Mounier, S. Richard, and P.J. Sansonetti. 1987. In vitro model of penetration and intracellular growth of *Listeria monocytogenes* in the human enterocyte-like cell line Caco-2. *Infect. Immun.* 55:2822–2829.
13. Halbrugge, M., and U. Walter. 1990. Analysis, purification and properties of a 50,000-dalton membrane-associated phosphoprotein from human platelets. *J. Chromatogr.* 521:335–343.
14. Headley, V.L. and S.M. Payne. 1990. Differential protein expression by *Shigella flexneri* in intracellular and extracellular environments. *Proc. Natl. Acad. Sci. USA.* 87:4179–4183.
15. Heinzen, R.A., S.F. Hayes, M.G. Peacock, and T. Hackstadt. 1993. Directional actin polymerization associated with spotted fever group *Rickettsia* infection of Vero cells. *Infect. Immun.* 61:1926–1935.
16. Horton, R.M., Z. Cai, S.N. Ho, and L.R. Pease. 1990. Gene splicing by overlap extension: tailor-made genes using the polymerase chain reaction. *Biotechniques.* 8:528–535.
17. Kocks, C., E. Gouin, M. Tabouret, P. Berche, H. Ohayon, and P. Cossart. 1992. *L. monocytogenes*-induced actin assembly requires the *actA* gene product, a surface protein. *Cell.* 68:521–531.
18. Kocks, C., R. Hellio, P. Gounon, H. Ohayon, and P. Cossart. 1993. Polarized distribution of *Listeria monocytogenes* surface protein ActA at the site of directional actin assembly. *J. Cell Sci.* 105:699–710.
19. Kocks, C., J.-B. Marchand, E. Gouin, H. d'Hauteville, P.J. Sansonetti, M.-F. Carlier, and P. Cossart. 1995. The unrelated surface proteins ActA of *Listeria monocytogenes* and IcsA of *Shigella flexneri* are sufficient to confer actin-based motility on *Listeria innocua* and *Escherichia coli* respectively. *Mol. Microbiol.* 18:413–423.
20. Kuhn, M., M.-C. Prévost, J. Mounier, and P.J. Sansonetti. 1990. A nonvirulent mutant of *Listeria monocytogenes* does not move intracellularly but still induces polymerization of actin. *Infect. Immun.* 58:3477–3486.
21. Lasa, I., V. David, E. Gouin, J.-B. Marchand, and P. Cossart. 1995. The amino-terminal part of ActA is critical for the actin-based motility of *Listeria monocytogenes*; the central proline-rich region acts as a stimulator. *Mol. Microbiol.* 18:425–436.
22. Machesky, L.M. and T.D. Pollard. 1993. Profilin as a potential mediator of membrane-cytoskeleton communication. *Trends Cell Biol.* 3:381–385.
23. Marchand, J.B., P. Moreau, A. Paoletti, P. Cossart, M.-F. Carlier, and D. Pantaloni. 1995. Actin-based movement of *Listeria monocytogenes*: actin assembly results from the local maintenance of uncapped filament barbed ends at the bacterium surface. *J. Cell Biol.* 130:331–343.
24. Mounier, J., A. Ryter, M. Coquis-Rondon, and P.J. Sansonetti. 1990. Intracellular and cell-to-cell spread of *Listeria monocytogenes* involves interaction with F-actin in the enterocytelike cell line Caco-2. *Infect. Immun.* 58:1048–1058.
25. Murray, A.W. 1991. Cell cycle extracts. *Methods Cell Biol.* 36:581–605.
26. Nachmias, V.T. 1993. Small actin-binding proteins: the β-thymosin family. *Curr. Biol.* 5:56–62.
27. Pantaloni, D., and M.-F. Carlier. 1993. How profilin promotes actin filament assembly in the presence of thymosin β4. *Cell.* 75:1007–1014.
28. Pistor, S., T. Chakraborty, K. Niebuhr, E. Domann, and J. Wehland. 1994. The ActA protein of *Listeria monocytogenes* acts as a nucleator inducing reorganization of the actin cytoskeleton. *EMBO (Eur. Mol. Biol. Organ.) J.* 13:758–763.
29. Pistor, S., T. Chakraborty, U. Walter, and J. Wehland. 1995. The bacterial actin nucleator protein ActA of *Listeria monocytogenes* contains multiple binding sites for host microfilament proteins. *Curr. Biol.* 5:517–525.
30. Pollard, T.D. 1994. Structure of actin binding proteins: insights about function at atomic resolution. *Annu. Rev. Cell Biol.* 10:207–249.

31. Portnoy, D.A. 1992. Innate immunity to a facultative intracellular bacterial pathogen. *Curr. Opin. Immunol.* 4:20–24.
32. Portnoy, D.A., P.S. Jacks, and D.J. Hinrichs. 1988. Role of hemolysin for the intracellular growth of *Listeria monocytogenes*. *J. Exp. Med.* 167: 1459–1471.
33. Pring, M., A. Weber, and M.R. Bubb. 1992. Profilin-actin complexes directly elongate actin filaments at the barbed end. *Biochemistry.* 31:1827–1836.
34. Reinhard, M., K. Giehl, K. Abel, C. Haffner, T. Jarchau, V. Hoppe, B.M. Jockusch, and U. Walter. 1995. The proline-rich focal adhesion and microfilament protein VASP is a ligand for profilins. *EMBO (Eur. Mol. Biol. Organ.) J.* 14:19–27.
35. Sadler, I., A.W. Crawford, J.W. Michelsen, and M.C. Beckerle. 1992. Zyxin and cCRP: two interactive LIM domain proteins associated with the cytoskeleton. *J. Cell Biol.* 119:1573–1587.
36. Sanger, J.M., J.W. Sanger, and F.S. Southwick. 1992. Host cell actin assembly is necessary and likely to provide the propulsive force for intraceullar movement of *Listeria monocytogenes*. *Infect. Immun.* 60:3609–3619.
37. Smith, G.A., H. Marquis, S. Jones, N.C. Johnston, D.A. Portnoy, and H. Goldfine. 1995. The two distinct phospholipases C of *Listeria monocytogenes* have overlapping roles in escape from a vacuole and cell-to-cell spread. *Infect. Immun.* 63:4231–4237.
38. Smith, G.A., D.A. Portnoy, and J.A. Theriot. 1995. Asymmetric distribution of the *Listeria monocytogenes* ActA protein is required and sufficient to direct actin-based motility. *Mol. Microbiol.* 17:945–951.
39. Smith, K., and P. Youngman. 1992. Use of a new integrational vector to investigate compartment-specific expression of the *Bacillus subtilis spoIIM* gene. *Biochimie (Paris).* 74:705–711.
40. Southwick, F.S., and D.L. Purich. 1994. Arrest of *Listeria* movement in host cells by a bacterial ActA analogue: implications for actin-based motility. *Proc. Natl. Acad. Sci. USA.* 91:5168–5172.
41. Sun, A.N., A. Camilli, and D.A. Portnoy. 1990. Isolation of *Listeria monocytogenes* small-plaque mutants defective for intracellular growth and cell-to-cell spread. *Infect. Immun.* 58:3770–3778.
42. Tanaka, M., and H. Shibata. 1985. Poly(L-proline)-binding proteins from chick embryos are a profilin and a profilactin. *Eur. J. Biochem.* 151:291–297.
43. Teysseire, N., C. Chiche-Portiche, and D. Raoult. 1992. Intracellular movements of *Rickettsia conorii* and *R. typhi* based on actin polymerization. *Res. Microbiol.* 143:821–829.
44. Theriot, J.A., and T.J. Mitchison. 1993. The three faces of profilin. *Cell.* 75: 835–838.
45. Theriot, J.A., T.J. Mitchison, L.G. Tilney, and D.A. Portnoy. 1992. The rate of actin-based motility of intracellular *Listeria monocytogenes* equals the rate of actin polymerization. *Nature (Lond.).* 357:257–260.
46. Theriot, J.A., J. Rosenblatt, D.A. Portnoy, P.J. Goldschmidt-Clermont, and T. J. Mitchison. 1994. Involvement of profilin in the actin-based motility of *L. monocytogenes* in cells and cell-free extracts. *Cell.* 76:505–517.
47. Tilney, L.G., and D.A. Portnoy. 1989. Actin filaments and the growth, movement, and spread of the intracellular bacterial parasite, *Listeria monocytogenes*. *J. Cell Biol.* 109:1597–1608.
48. Tilney, L.G., P.S. Connelly, and D.A. Portnoy. 1990. Actin filament nucleation by the bacterial pathogen, *Listeria monocytogenes*. *J. Cell Biol.* 111: 2979–2988.
49. Tilney, L.G., D.J. DeRosier, and M.S. Tilney. 1992. How *Listeria* exploits host cell actin to form its own cytoskeleton. I. Formation of a tail and how that tail might be involved in movement. *J. Cell Biol.* 118:71–81.
50. Tilney, L.G., D.J. DeRosier, A. Weber, and M.S. Tilney. 1992. How *Listeria* exploits host cell actin to form its own cytoskeleton. II. Nucleation, actin filament polarity, filament assembly, and evidence for a pointed end capper. *J. Cell Biol.* 118:83–93.
51. Tomasz, A. 1981. Surface components of *Streptococcus pneumoniae*. *Rev. Inf. Dis.* 3:190–211.
52. Williamson, M.P. 1994. The structure and function of proline-rich regions in proteins. *Biochem. J.* 297:249–260.
53. Zhukarev, V., F. Ashton, J.M. Sanger, J.W. Sanger, and H. Shuman. 1995. Organization and structure of actin filament bundles in *Listeria*-infected cells. *Cell Motil. Cytoskel.* 30:229–246.
54. Zigmond, S.H. 1993. Recent quantitative studies of actin filament turnover during cell locomotion. *Cell Motil. Cytoskeleton.* 25:309–316.